2017

Stable and Radiocarbon Isotopic Composition of Dissolved Organic Matter in the Gulf of Mexico

B. D. Walker
Keck Carbon Cycle AMS Laboratory

E. R. M. Druffel
Keck Carbon Cycle AMS Laboratory

J. Kolasinski
University of South Florida

B. J. Roberts
Universities Marine Consortium

X. Xu
Keck Carbon Cycle AMS Laboratory

See next page for additional authors

AGU PUBLICATIONS

Geophysical Research Letters

RESEARCH LETTER
10.1002/2017GL074155

Key Points:
- Mississippi River DOC carries terrestrial "bomb" ^{14}C, which is removed and recycled offshore with advection of the river plume
- Deep Gulf of Mexico (GOM) DOC ^{14}C is higher than deep Caribbean feed water, suggesting a modern DOC source in the deep GOM basin
- High mesopelagic DOC and low ^{13}C and ^{14}C values southwest of the Macondo Wellhead suggest long-term persistence of petrocarbon as DOC

Supporting Information:
- Supporting Information S1

Correspondence to:
B. D. Walker,
brett.walker@uci.edu

Citation:
Walker, B. D., E. R. M. Druffel, J. Kolasinski, B. J. Roberts, X. Xu, and B. E. Rosenheim (2017), Stable and radiocarbon isotopic composition of dissolved organic matter in the Gulf of Mexico, *Geophys. Res. Lett.*, *44*, 8424–8434, doi:10.1002/2017GL074155.

Received 12 MAY 2017
Accepted 25 JUL 2017
Accepted article online 3 AUG 2017
Published online 17 AUG 2017

Stable and radiocarbon isotopic composition of dissolved organic matter in the Gulf of Mexico

B. D. Walker[1], E. R. M. Druffel[1], J. Kolasinski[2,3,4], B. J. Roberts[5], X. Xu[1], and B. E. Rosenheim[2,3]

[1]Department of Earth System Science, Keck Carbon Cycle AMS Laboratory, Irvine, California, USA, [2]College of Marine Science, University of South Florida, St. Petersburg, Florida, USA, [3]Earth and Environmental Sciences, Tulane University of Louisiana, New Orleans, Louisiana, USA, [4]Now at UMR ENTROPIE, Labex Corail, Université de La Réunion, St Denis, France, [5]DeFelice Marine Center, Louisiana Universities Marine Consortium, Chauvin, Louisiana, USA

Abstract Dissolved organic carbon (DOC) is of primary importance to marine ecosystems and the global carbon cycle. Stable carbon ($\delta^{13}C$) and radiocarbon ($\Delta^{14}C$) isotopic measurements are powerful tools for evaluating DOC sources and cycling. However, the isotopic signature of DOC in the Gulf of Mexico (GOM) remains almost completely unknown. Here we present the first DOC $\Delta^{14}C$ and $\delta^{13}C$ depth profiles from the GOM. Our results suggest the Mississippi River exports large amounts of DOC with an anthropogenic "bomb" $\Delta^{14}C$ signature. Riverine DOC is removed and recycled offshore, and some marine production of DOC is observed in the river plume. Offshore profiles show that DOC has higher $\Delta^{14}C$ than its Caribbean feed waters, indicative of a modern deep DOC source in the GOM basin. Finally, high DOC with negative $\delta^{13}C$ and $\Delta^{14}C$ values were observed near the Macondo Wellhead, suggesting a transformation of Deepwater Horizon hydrocarbons into a persistent population of DOC.

Plain Language Summary The Deepwater Horizon (DWH) spill released 4.1–4.6 million barrels of oil over 87 days to the deep Gulf of Mexico (GOM) and is considered one of humankind's largest environmental disasters. Now, 7 years after DWH, a significant portion of this oil (10–25%) remains unaccounted for. We estimate that 10–16% of DWH hydrocarbon has been incorporated into marine dissolved organic carbon (DOC)—the largest organic C reservoir in the ocean. Our results suggest that natural GOM bacteria transformed much of the spilled petroleum and methane into natural DOC molecules, effectively dissolving this C into deep ocean water. Our results also highlight the dynamic cycling of DOC in the GOM basin—including the rapid removal of modern Mississippi River C as its plume moves offshore and a modern C contribution to the deep GOM DOC reservoir.

1. Introduction

The Gulf of Mexico (GOM) has an ocean surface area of ~1.6×10^6 km^2 and has an average depth of ~3800 m. Despite its small size, the GOM comprises a globally significant commercial fishery because of its highly productive waters. Water entering the GOM through the Yucatán Channel (~2040 m) is roughly equal to that exiting the GOM in the Florida Current via the Florida Straits (740 m), with current flows of 30.0 ± 5.3 sverdrup (Sv) and 30.8 ± 3.2 Sv, respectively [*Rousset and Beal*, 2010, 2014]. Deep water in the GOM is predominantly North Atlantic Deep Water (NADW) that spills over the Yucatán Sill. The ventilation age of deep waters in the GOM has been estimated to be ~250 years [*Rivas et al.*, 2005].

At the true base of the oceanic food web, dissolved organic carbon (DOC: ~662 GtC) is of primary importance to marine ecosystems and the global carbon cycle [*Hansell et al.*, 2009]. Stable ($\delta^{13}C$) and radiocarbon ($\Delta^{14}C$) isotopic measurements are powerful tools for evaluating DOC sources and cycling in aquatic environments [*Beaupre*, 2015; *Canuel and Hardison*, 2016; *McNichol and Aluwihare*, 2007]. However, the biogeochemistry of DOC in the broader Gulf of Mexico (GOM) basin remains largely unconstrained. In particular, the $\Delta^{14}C$ and $\delta^{13}C$ isotopic signature of DOC in the GOM is almost completely unknown.

The northern GOM is one of the world's most productive ocean margin regions and is an especially dynamic region for organic matter cycling. The Mississippi-Atchafalaya River system (MARS) drains approximately 41% of the lower 48 states and delivers approximately 80% of the freshwater and 91% of the estimated annual nitrogen load to the northern Gulf of Mexico [*Dunn*, 1996]. Previous work evaluating the isotopic composition and biological reactivity of high molecular weight (HMW; >1 kDa) DOC in the MARS and northern GOM found that HMW DOC is an important C source (polysaccharides) fueling bacterial production and is rapidly recycled

[*Gardner et al.*, 1996; *Guo et al.*, 2009; *Santschi et al.*, 1995]. The MARS also delivers significant quantities of dissolved organic matter (DOM) to the northern GOM [*Bianchi et al.*, 2004; *Shen et al.*, 2012]. This large, episodic delivery of terrestrial DOC (tDOC) from this river system is rapidly removed in the northern GOM [*Bianchi et al.*, 2004; *Fichot et al.*, 2014]. It is estimated that ~40% of this tDOC is remineralized to CO_2 on the Louisiana shelf [*Fichot and Benner*, 2014]. Recent work has also observed that phytoplankton and microbial communities produce "hot spots" of labile DOM at intermediate salinities along the northern GOM shelf regions, which is subsequently exported offshore as semilabile DOM. Microbial alteration of this DOM can result in the seasonal accumulation of 0.11–0.23 Tg DOC [*Shen et al.*, 2016]. Slope regions in the northern GOM are also populated with many methane and hydrocarbon seeps, which can be observed in the surface as "slicks" and have been associated with high phytoplankton biomass [*D'Souza et al.*, 2016; *MacDonald et al.*, 2015]. Natural seeps may comprise a source of ancient DOC to the deep GOM [*Pohlman et al.*, 2011; *Pohlman et al.*, 2009]; however, the long-term persistence of natural hydrocarbon seep DOC in the GOM is unknown. The Deepwater Horizon (DWH) spill event in 2010 has also complicated our knowledge of DOM cycling in the GOM, because baseline measurements of DOC prior to the spill are scarce. In addition, the long-term geochemical impact of DWH on the deep DOC reservoir remains largely unknown.

Here we report DOC $\Delta^{14}C$ and $\delta^{13}C$ profiles from several regions in the northern GOM: (1) the Mississippi River mouth (MR), (2) its aging river plume (MRP), (3) the shelf/slope near the Macondo Wellhead site (MWS), (4) the offshore Loop Current (LC), and (5) a nearshore mesoscale Loop Current eddy (LCE). We first discuss DOC export and cycling at the Mississippi R. and GOM interface. Second, we discuss the long-term geochemical impact of the DWH spill event on the DOC pool as revealed by profiles taken close the MWS. Finally, we examine an offshore DOC $\Delta^{14}C$ and $\delta^{13}C$ profile in the context of Caribbean waters feeding the GOM basin, to evaluate DOC cycling in the deep GOM.

2. Materials and Methods

Samples were obtained from the northern Gulf of Mexico during a Consortium for Advanced Research on Hydrocarbon Transport in the Environment (CARTHE) pelagic sampling and observation expedition aboard the R/V *Pelican* (PE1501; July 2014) and also during a Global Ocean Ship-based Hydrographic Investigations Program (GO-SHIP) Repeat Hydrography cruise in the North Atlantic (A20, Station 27, April 2012; 12.75°N, 52.33°W). Samples from the northern GOM were taken from six stations: P1 = MR, P2 = MRP, P3 = MWS, S4 = MWS/LC, P4 = LC, and P5 = LCE (Figure 1).

All glassware used in this study was acid cleaned (10% HCl), rinsed with 18.2 MΩ Milli-Q water, and combusted at 540°C for 2 h prior to sample collection. Seawater DOC samples were collected into 1 L Amber Boston Round bottles with acid cleaned Teflon® lined caps from the Niskin bottle rosette and stored frozen at −20°C prior to analysis. Samples were filtered (0.8 μm QMA, 70 mm diameter) using an acid cleaned stainless steel manifold and silicone tubing only for depths shallower than 400 m. For details pertaining to ancillary nutrient and dissolved inorganic carbon (DIC) isotopic analysis, we refer the reader to the supporting information (see section S3).

We use the dilution method for UV photo-oxidation (UVox) isolation of seawater DOC [*Beaupre et al.*, 2007; *Griffin et al.*, 2010]. DOC samples (~800 mL) are diluted to a final volume of ~1000 mL with 18.2 MΩ Milli-Q water (MQ DOC = 0.5–1.0 μM) prior to oxidation. The volumes of sample and MQ water are measured using a calibrated cathetometer in a quartz reactor and acidified with 1 mL 85% phosphoric acid. Dissolved inorganic carbon (DIC) is sparged from the sample using ultra high purity (5.0) helium, then the DOC is oxidized to CO_2 using a 1200 W medium-pressure, mercury arc UV lamp for 4 h. The CO_2 evolved is then sparged with ultrahigh purity (5.0) helium, purified cryogenically, and manometrically quantified. Two DOC sample replicates (Station P3 at 1000 m and Station P4 at 1500 m) yielded concentrations within 0.7 μM and 1.25 μM (Table S1). This is consistent with previous work [*Druffel et al.*, 2013; *Walker et al.*, 2016a] demonstrating average procedural reproducibility of UVox DOC concentrations using this system to be ±1.1 μM. Separate aliquots of the CO_2 are analyzed for $\delta^{13}C$ and $\Delta^{14}C$ using standard techniques [*Southon et al.*, 2004; *Vogel et al.*, 1987].

Following production of CO_2, carbon yields were measured manometrically and aliquots taken for $\Delta^{14}C$ and $\delta^{13}C$ analyses. CO_2 was converted to graphite using either the H_2 or Zn method [*Vogel et al.*, 1987; *Xu et al.*, 2007]. Radiocarbon measurements for all samples are reported as $\Delta^{14}C$ in per mil (‰) and are

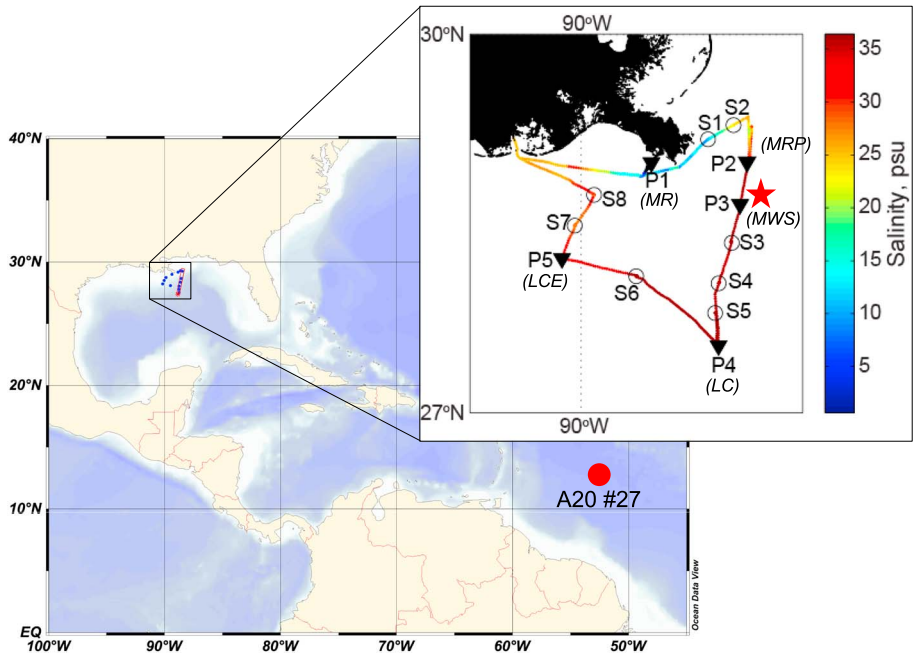

Figure 1. Site map of all sample locations for CARTHE Pelagic Sampling Cruise (PE15-01, R/V *Pelican*, July 2014). Outlined by the rectangle are GOM sampling stations (upper right). DOC concentration, $\Delta^{14}C$, and $\delta^{13}C$ samples were taken from stations P3, S4, and P4; ancillary hydrographic data and nutrients were taken from all stations (supporting information). The location of the Macondo Well head is indicated by a red star. Colors indicate surface salinity values measured along the cruise track and indicate the Mississippi River plume (P1 and S1) and high salinity Loop Current waters (P4). The Caribbean Sea station is indicated by a red circle (GO-SHIP A20, R/V *Atlantis*, May 2012, Station 27; 13°N, 52°W). Italicized station descriptors (see text) are also indicated in parentheses.

corrected for extraneous C introduced during processing using small standards and backgrounds of known ^{14}C content. The ^{14}C analyses of DOC samples (~50–800 μgC) recovered from these procedures were performed at the Keck Carbon Cycle AMS (KCCAMS) Laboratory at UCI. Samples are reported with a total uncertainty of ±4‰.

Equilibrated splits of DOC CO_2 gas were also cryogenically transferred to 3 mm diameter, 60 mm length Pyrex tubes using liquid N_2 and sealed under vacuum for $\delta^{13}C$ analysis. These 3 mm Pyrex tubes were then scored with a glass cutter, placed into Exetainer® vials with two 8 mm solid glass marbles, inverted and purged for 20 s in a glove bag, flushed with ultrahigh purity (5.0) helium and capped. CO_2 in the Pyrex tube was released into the Exetainer vial when the tube was broken by shaking the marbles. DOC $\delta^{13}C$ values were then measured at the KCCAMS Laboratory using a Gas Bench II and a Finnigan Delta Plus isotope ratio mass spectrometer at UCI, with an analytical uncertainty of ±0.2‰.

We use two simple modeling approaches for evaluating DOC cycling, as revealed by $\Delta^{14}C$ and $\delta^{13}C$ values, in the GOM. First, we use conservative two-end-member salinity (S) mixing of riverine (r = P1, 1 m) versus seawater (sw = P3, 26 m) end-members to constrain their contributions (f) to both deep MR and surface MRP samples:

$$f_{\text{sample}}\, S_{\text{sample}} = f_r\, S_r + f_{\text{sw}}\, S_{\text{sw}} \tag{1}$$

where $f_r + f_{\text{sw}} = 1$. A set of equations ((2)–(4)) were then used to predict expected DOC concentrations, $\Delta^{14}C$, and $\delta^{13}C$ values based on conservative salinity mixing (Figure S10), again where $f_r + f_{\text{sw}} = 1$.

$$\text{DOC}_{\text{expected}} = f_r\, \text{DOC}_r + f_{\text{sw}}\, \text{DOC}_{\text{sw}} \tag{2}$$

$$\Delta^{14}\text{C}_{\text{expected}} = f_r\, \Delta^{14}\text{C}_r + f_{\text{sw}}\, \Delta^{14}\text{C}_{\text{sw}} \tag{3}$$

$$\delta^{13}\text{C}_{\text{expected}} = f_r\, \delta^{13}\text{C}_r + f_{\text{sw}}\, \delta^{13}\text{C}_{\text{sw}} \tag{4}$$

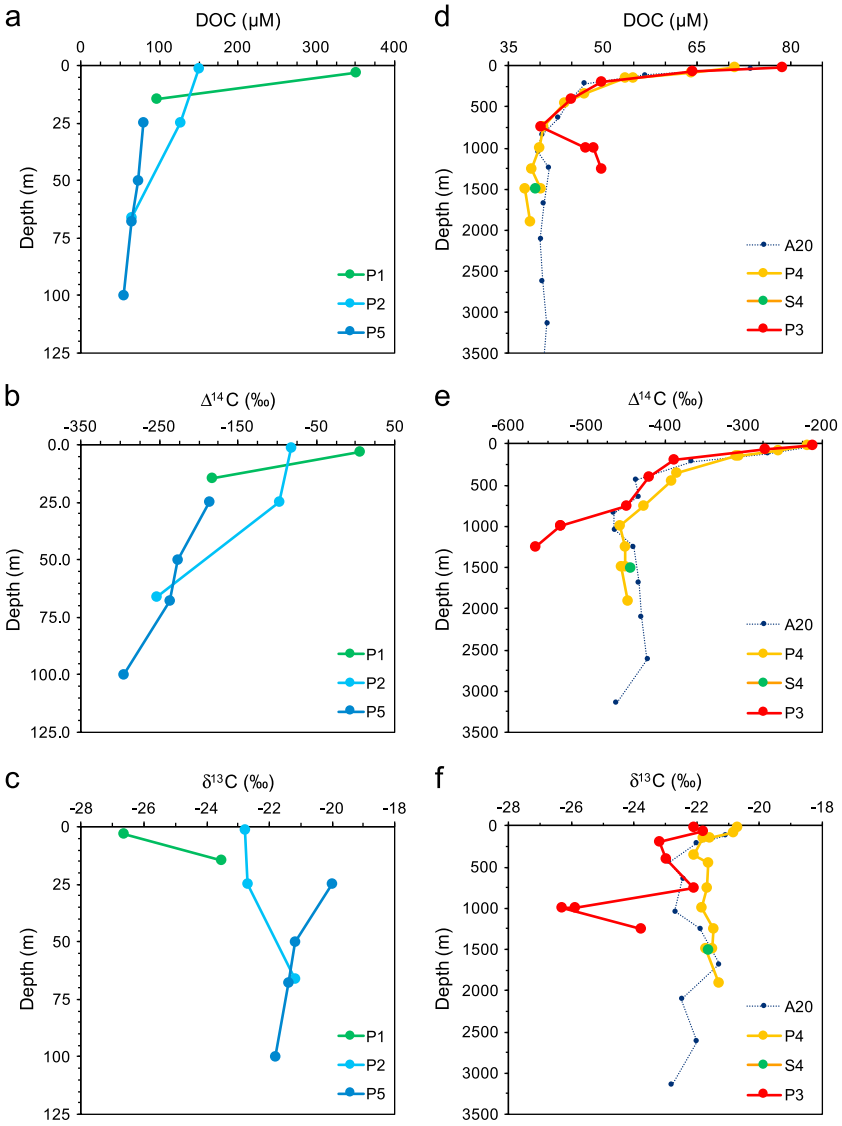

Figure 2. Dissolved organic carbon (DOC) concentrations together with stable carbon ($\delta^{13}C$) and radiocarbon ($\Delta^{14}C$) isotopic values clearly indicate the presence of excess petrocarbon DOC at the Macondo wellhead site (P3; 28.65°N) and offshore (P4; 27.53°N) values similar to the Caribbean Sea (A20). Plots are divided into nearshore (left: P1, P2, and P5) and offshore (P3, S4, P4, and A20) columns. (a, d) DOC concentrations (μM); (b, e) $\Delta^{14}C$ and (c, f) $\delta^{13}C$ values. For all plots, measurement uncertainties are smaller than the symbols. Please note DOC and $\Delta^{14}C$ *x* axis scales differ for nearshore and offshore plots.

Second, we use an isotopic mass balance for determining the isotopic composition of the DOC "added" causing a deviation from conservative mixing:

$$\Delta\mathrm{DOC} = \mathrm{DOC}_{\mathrm{measured}} - \mathrm{DOC}_{\mathrm{expected}} \tag{5}$$

where ΔDOC is the amount of DOC added (μM) and $\mathrm{DOC}_{\mathrm{measured}}$ and $\mathrm{DOC}_{\mathrm{expected}}$ are our actual measured values and expected values based on salinity mixing, respectively. We then assume our measured $\Delta^{14}C$ values comprise a mixture of this added DOC and that expected via salinity mixing:

$$\mathrm{DOC}_{\mathrm{measured}}\,\Delta^{14}\mathrm{C}_{\mathrm{measured}} = \mathrm{DOC}_{\mathrm{expected}}\,\Delta^{14}\mathrm{C}_{\mathrm{expected}} + \mathrm{DOC}_{\mathrm{added}}\,\Delta^{14}\mathrm{C}_{\mathrm{added}} \tag{6}$$

and solving for $\Delta^{14}C_{added}$:

$$\Delta^{14}\mathrm{C}_{\mathrm{added}} = \left[\left(\mathrm{DOC}_{\mathrm{measured}}\,\Delta^{14}\mathrm{C}_{\mathrm{measured}}\right) - \left(\mathrm{DOC}_{\mathrm{expected}}\,\Delta^{14}\mathrm{C}_{\mathrm{expected}}\right)\right]/\mathrm{DOC}_{\mathrm{added}} \tag{7}$$

For $\delta^{13}C_{added}$, an analogous expression was used. Below, we describe any changes in DOC concentrations, $\Delta^{14}C$, and $\delta^{13}C$ isotopic values (either between two measured values or isotopic mass balance versus measured values) as ΔDOC, $\Delta\Delta^{14}C$, and $\Delta\delta^{13}C$, respectively. All errors were propagated using known measurement uncertainties [*Taylor*, 1997]. For more detail on these calculations, see supporting information section S3.3.

3. Results and Discussion

A summary of measured northern GOM DOC concentrations, $\Delta^{14}C$, and $\delta^{13}C$ values is provided in Table S1 and is also shown as station depth profiles in Figures 2a–2f. Here we discuss these results in the context of DOC cycling within (1) the MR, (2) the aging MRP, (3) the long-term geochemical impacts of DWH on the DOC reservoir at the MWS, and (4) DOC cycling within the broader GOM basin by comparing LC and LCE profiles to previously measured values from the Caribbean.

3.1. Terrestrial DOC Export From the Mississippi River

Previous work has characterized the variability of DOC concentrations and $\delta^{13}C$ values in the Mississippi River [e.g., *Bianchi et al.*, 2004; *Duan et al.*, 2007] and the isotopic composition ($\Delta^{14}C$, $\delta^{13}C$, and $\delta^{15}N$) of HMW DOM in the Mississippi River and Northern GOM [*Guo et al.*, 2009]. However, to the best of our knowledge, total seawater DOC $\Delta^{14}C$ values for the MR have not been reported. We measured total DOC concentration, $\Delta^{14}C$, and $\delta^{13}C$ from the MR (Station P1) at two depths (1 and 15 m). The two depths correspond to the freshwater/saltwater end-members above and below the sharp halocline of the estuarine salt wedge. Surface MR water (S = 1.48) contained high DOC (350 μM), high $\Delta^{14}C$ (+5‰), and low $\delta^{13}C$ (−26.7‰) values (Table S1 and Figures 2a–2c). In contrast, deep MR water (S = 34.9) had lower DOC (96 μM), a lower $\Delta^{14}C$ value (−183‰), and a higher $\delta^{13}C$ value (−23.5‰).

We observe a large DOC offset (ΔDOC = 254 μM) between surface and deep MR. This DOC offset is not due to simple vertical mixing across the halocline but instead is primarily caused by the intrusion of offshore seawater with some minor input of surface MR water. Based on conservative salinity mixing (equation (1)) of surface MR (S = 1.48) with offshore seawater beyond the river plume influence (P3 26 m, S = 36.07), we determine that deep MR (S = 34.92) is composed of 3.3 ± 0.1% freshwater and 96.7 ± 0.1% seawater. Using these contributions, a simple DOC and isotopic mass balance of surface MR and surface offshore water (P3 26 m) suggests deep MR should have DOC = 87.6 ± 1.1 μM, $\Delta^{14}C$ = −205 ± 4‰, and $\delta^{13}C$ = −22.3 ± 0.2‰ (Figure S10 and supporting information section S3.3). These mass balance deep MR values are generally similar to our measured values, suggesting that the sharp change in DOC and its isotopic composition below the halocline is primarily attributed to estuarine mixing with offshore seawater. However, this simple mixing model (equations (2)–(4)) slightly underestimates deep MR DOC (ΔDOC = 9.1 μM) and yields a lower $\Delta^{14}C$ ($\Delta\Delta^{14}C$ = 22‰) value and higher $\delta^{13}C$ ($\Delta\delta^{13}C$ = 1.3‰) value, possibly indicating a small benthic MR contribution of negative $\Delta^{14}C$ and $\delta^{13}C$ DOC.

The difference between our mixing model and observed deep MR values may result from some production of DOC in the salt wedge, possibly at the halocline. A DOC isotopic mass of our salinity-based mixing estimate versus measured deep MR values (equations (5)–(7)) determines an additional 8.2 ± 1.0 μM DOC is added to the deep MR with $\Delta^{14}C$ = +47 ± 66‰ and $\delta^{13}C$ = −37 ± 4‰. It is interesting to note that these $\delta^{13}C$ values are consistent with an in situ biogenic (modern) methanogenic source of DOC below the MR halocline. More work is needed to precisely quantify the processes shaping DOC isotopic signatures within the Mississippi River and differences observed between conservative mixing calculations and measured deep MR values.

Overall, high MR DOC concentrations, low $\delta^{13}C$ values, and high $\Delta^{14}C$ values are consistent with the export of tDOC with an anthropogenic "bomb" $\Delta^{14}C$ signature to the GOM. We only have MR samples from one time and location. However, given previous observations of high DOC concentration variability in the Mississippi River [e.g., *Bianchi et al.*, 2004], we hypothesize that DOC $\Delta^{14}C$ and $\delta^{13}C$ values will also be temporally variable based on physical processes in the river (i.e., flow stage and tides). Our MR DOC samples were taken during high tide on 7 July 2014, during a period of climatologically average river flow (Figure S1). Thus, our DOC, $\Delta^{14}C$, and $\delta^{13}C$ values can only be interpreted to represent the Mississippi River during similar river seasonal flow and tidal conditions.

3.2. DOC Isotopic Signature of the Aged Mississippi River Plume

The predominant direction of the MRP in the northern GOM is to the southwest, however, during our cruise the MRP was observed to the northeast via satellite and compiled buoy observations used by the Navy Coastal Ocean Salinity Model (F. E. Muller-Karger, personal communication, 2014). Here we discuss a shallow DOC $\Delta^{14}C$ and $\delta^{13}C$ depth profile (66 m) located at the oceanic front of the aged MRP (Station P2). As for the MR, the two surface MRP samples (2 and 26 m; S = 31.53 and 36.29) contained both high DOC (150 μM, 126 μM; Figure 2a) and high $\Delta^{14}C$ values (−82‰ and −97‰; Figure 2b). These surface MRP samples had nearly identical $\delta^{13}C$ values (−22.8‰, −22.7‰; Figure 2c) that are only slightly negative with respect to the offshore marine $\delta^{13}C$ end-member (Stations P3 and P4 $\delta^{13}C$ = −22.1‰ and −20.7‰, respectively). In contrast, the deepest MRP sample (66 m) had DOC (64 μM) and isotopic values ($\Delta^{14}C$ = −254‰ and $\delta^{13}C$ = −21.2‰) more consistent with those observed at similar depths offshore (Stations P3 and P4), suggesting that only the surface <30 m of Station P2 were influenced by tDOC within the MRP.

A simple salinity mixing model (equation (1)), suggests that the 2 m MRP sample is composed of 13.1 ± 0.1% MR water and 86.9 ± 0.1% seawater. Using the DOC abundance and $\Delta^{14}C$ and $\delta^{13}C$ isotopic signatures of these end-members (equations (2)–(4)), a S = 31.53 predicts MRP 2 m DOC = 114.2 ± 1.0 μM with $\Delta^{14}C$ = −184 ± 4‰ and $\delta^{13}C$ = −22.7 ± 0.2‰. The salinity mixing calculation accurately predicts the $\delta^{13}C$ signature but predicts lower DOC (ΔDOC = 36.1 μM) and a lower $\Delta^{14}C$ value ($\Delta\Delta^{14}C$ = −94‰). This simple mixing model does not account for known major DOC removal mechanisms occurring in the MRP (e.g., flocculation, microbial remineralization, and photo-oxidation). Thus, an isotopic mass balance of the salinity mixing estimate versus our measured DOC values (equations (5)–(7)) indicates there must be substantial excess DOC production (36.2 ± 1.0 μM) with anthropogenic bomb C ($\Delta^{14}C$ = 206 ± 14‰) within the aged MRP, presumably via marine primary production. Interestingly, the 26 m sample at P2 has a salinity similar to that of P3 (S = 36.29 versus 36.07). Thus, the ΔDOC = 48 μM between P2, 26 m and offshore P3 waters at the same depth (79 μM) likely results from the accumulation *marine* DOC (as opposed to a removal of tDOC) with low $\Delta^{14}C$ signatures during microbial alteration of DOC in biological "hot spots" on the shelf [*Shen et al.*, 2016].

3.3. Long-Term Geochemical Impact of Deepwater Horizon on the GOM DOC Reservoir

Along the offshore surface transect (Stations P3, S4, and P4) DOC concentrations ranged from 71 to 79 μM (~25 m) and $\Delta^{14}C$ values ranged from −212‰ to −274‰ at depths <100 m (Figures 2d and 2e). Typical marine DOC $\delta^{13}C$ values (−20 to −22‰) were also observed in the surface (Figure 2f), with Station P3 $\delta^{13}C$ values slightly lower (−22.5‰ SD ± 0.6‰, n = 3) than those at Station P4 (−21.2‰, SD ± 0.5‰, n = 4). Deep DOC concentrations, $\Delta^{14}C$ and $\delta^{13}C$ values for Stations S4 and P4 were similar below 1000 m, averaging 39.2 ± 1.1 μM, $\Delta^{14}C$ = −449 ± 11‰, and $\delta^{13}C$ = −21.6 ± 0.2‰ (n = 7). In contrast, Station P3 (~20 km southwest of the MWS) showed a wider range in DOC concentrations (40.0 to 49.7 μM), $\Delta^{14}C$ (−449‰ to −566‰) and $\delta^{13}C$ (−22.1 to −26.3‰) values. The two deepest Station P3 samples, at 1000 m and 1250 m, had large DOC concentration and isotopic offsets in comparison to "background" deep Station P4 sample values (ΔDOC = +7.9 to +9.7 μM, $\Delta\Delta^{14}C$ = −75 to −120‰, and $\Delta\delta^{13}C$ = −2.2 to −4.4‰).

These large DOC concentration and carbon isotopic offsets at Station P3, in the mesopelagic depths southwest of the MWS, are both striking and unexpected (Figures 2d–2f and S2). The ~9 ± 1 μM increase in DOC between 750 m and 1000–1250 m with low $\Delta^{14}C$ and $\delta^{13}C$ values was not observed further offshore (P4). Filtered versus nonfiltered 1000 m duplicates at P3 have similar DOC concentrations and isotopic values, suggesting that P3 isotopic offsets cannot be attributed to particles. To the best of our knowledge, deep DOC increases of this nature have never been observed in the deep ocean. Together with the low $\Delta^{14}C$ and $\delta^{13}C$ values, these results suggest either that a 1000–1250 m northern GOM DOC anomaly persists as the result from incorporation of mesopelagic DWH plume petroleum carbon (petrocarbon) into DOC, or possibly an advection of benthic hydrocarbon seep DOC from the northern GOM slope. Using a simple $\Delta^{14}C$ and $\delta^{13}C$ isotopic mass balance, we estimate that at 1000 m there is an addition of 7.9 μM DOC with $\Delta^{14}C$ = −965 ± 85‰ and $\delta^{13}C$ = −44.6 ± 4.6‰ (above background DOC; DOC = 40 μM, $\Delta^{14}C$ = −449‰, and $\delta^{13}C$ = −22.1‰ at 750 m). Similarly, at 1250 m we estimate a DOC addition of 9.7 μM with $\Delta^{14}C$ = −1000‰ and $\delta^{13}C$ = −30.8 ± 3.6‰. Together, these results indicate a 19–24% increase in DOC as petrocarbon in the mesopelagic GOM at Station P3. Our $\Delta^{14}C$ isotopic mass balance suggests DOC petrocarbon (DOC_{pc}) added with similar $\Delta^{14}C$ value at each depth. In contrast, our $\delta^{13}C$ isotopic mass balance indicates

two distinct petrocarbon sources: At 1000 m, the added DOC_{pc} has a lower $\delta^{13}C$ signature, indicative of a predominantly fossil methane source ($\delta^{13}C = -60‰$), and at 1250 m, added DOC_{pc} has a higher $\delta^{13}C$ value indicative of a predominantly fossil oil source ($\delta^{13}C = -27‰$) [*Cherrier et al.*, 2014; *Graham et al.*, 2010].

Using an analogous approach to that of Cherrier and coworkers, we prescribe two petrocarbon $\delta^{13}C$ end-members in order to constrain the relative contributions of methane ($\delta^{13}C = -59 \pm 2‰$) versus Louisiana light crude oil ($\delta^{13}C = -27 \pm 0.4‰$) [*Cherrier et al.*, 2014; *Graham et al.*, 2010] to DOC_{pc} using the following relationship:

$$f_{pc}\,\delta^{13}C_{pc} = f_{oil}\,\delta^{13}C_{oil} + f_{methane}\,\delta^{13}C_{methane} \quad (8)$$

where f is the percent contribution of each end-member, $f_{oil} + f_{methane} = f_{pc} = 100\%$, and $\delta^{13}C_{pc}$ represents the $\delta^{13}C$ of DOC petrocarbon added. Using equation (8), we determine f_{oil} and $f_{methane}$ at 1000 m to account for 42% and 58% (±1% propagated error) of excess DOC_{pc}, respectively. In contrast, f_{oil} and $f_{methane}$ at 1250 m comprise 89% and 11% (±2%), respectively. These results highlight the contribution of both methane and crude oil to the DOC_{pc} plume at 1000 m. In contrast, at 1250 m only a minor methane and large oil DOC_{pc} contribution is observed. The disparate contribution of oil versus methane DOC_{pc} may be related to the physical partitioning of dispersed DWH hydrocarbons as a function of droplet size, chemistry, or phase [*Paris et al.*, 2012]. The relative distributions of oil and methane petrocarbon we observe are consistent with previous work evaluating the predominance of hydrocarbon gas (i.e., methane) at 800–1200 m and aromatic hydrocarbons (i.e., benzene) >1200 m immediately following the spill [*Camilli et al.*, 2010; *Kessler et al.*, 2011; *Reddy et al.*, 2012; *Valentine et al.*, 2010]. We note that the dispersant Corexit and other gases (<12% ethane and propane) were present in the water column [e.g., *Reddy et al.*, 2012] and are not included in the above contribution estimates.

In considering the physical mechanisms responsible for the DOC_{pc} anomalies we observe (i.e., degradation of a subsurface DWH plume versus natural seeps), it is important to consider all ancillary data and published research. For example, methane concentrations at P3 were negligible (Figure S3) and hydrocarbons (e.g., PAHs) from the DWH event are no longer present in the water column. In addition, our UVox DOC analysis does not isolate volatiles (e.g., methane). Thus, our low observed DOC_{pc} $\Delta^{14}C$ and $\delta^{13}C$ values must pertain to a natural population of DOC molecules that now carry a fossil (^{14}C-free) methane and oil isotopic signature.

We cannot completely rule out horizontal advection of benthic/sedimented oil and methane seep DOC to the midwater column at P3. However, this physical mechanism is difficult to reconcile with available data. Published work demonstrating such a mechanism is also lacking. Most studies focused on methane seep DOC have not observed significant seep-derived DOC beyond a few meters of the seep point source [*Pohlman et al.*, 2011; *Pohlman et al.*, 2009], suggesting that seep DOC is highly labile and rapidly recycled in the deep ocean. Station P3 is also not in the immediate vicinity of any vigorous hydrocarbon or methane seeps. An advection of benthic sediment/seep material is also not supported by our filtered versus nonfiltered 1000 m duplicates at P3 that yielded similar DOC concentrations and isotopic values. This comparison would seemingly preclude concurrent turbidity flows and/or sediment resuspension of DOC_{pc} sources. Our ancillary hydrographic data do not indicate sedimentary contributions at 1000 m and 1250 m at P3. We do not observe anomalously high methane, particulate organic carbon (POC), O_2, NO_3, NH_4, PO_4, and SiO_2 at P3 (see supporting information section S2.1). More work is needed to fully assess the midwater column GOM DOC_{pc} sources; however, given the available data, the most prudent explanation of the mesopelagic DOC_{pc} anomaly is a metabolic transformation of methane and hydrocarbons into the DOC reservoir during the intense microbial response and oxidation of the subsurface DWH methane and dispersed oil plume. We provide a brief discussion of the physical dispersion of the subsurface plume in the supporting information sections S2.1 and S2.2.

We hypothesize that this mesopelagic DOC_{pc} is biologically recalcitrant and may persist for many years. Previous work observed a rapid microbial metabolism and removal of methane and hydrocarbons from the subsurface DWH plume [*Camilli et al.*, 2010; *Crespo-Medina et al.*, 2014; *Joye et al.*, 2014; *Joye et al.*, 2011b; *Kessler et al.*, 2011; *Kleindienst et al.*, 2016; *Valentine et al.*, 2010]. However, no change in water mass properties, nutrients, and apparent oxygen utilization (AOU) along the transect (Figures S4–S6), in

combination with no correlation between deep DOC and either nutrients or AOU, suggests that rapid remineralization of this DOC_{pc} is no longer occurring. It is important to note that a change in AOU at these depths should not necessarily be expected given the decrease in observed dissolved oxygen anomalies within months following the microbial response to the spill [*Kessler et al.*, 2011]. If active remineralization of DOC_{pc} is no longer occurring, we hypothesize that physical dispersion (as opposed to biological remineralization) will be primarily responsible for future changes in elevated DOC concentrations in the mesopelagic GOM associated with the DWH event (see supporting information Figure S7). To date, not all of the 0.46–0.60 Tg of petrocarbon that was injected into the GOM from DWH [*Chanton et al.*, 2015; *Joye et al.*, 2011a] has been accounted for. Future work should focus on the role DOC_{pc} may play in closing the "missing" DWH oil spill budget. Our preliminary first-order estimate suggests that DOC_{pc} may comprise between 0.06 and 0.08 TgC, or ~10–16% of the oil spill budget (see supporting information section S2.2). We propose that this isotopically "labeled" DOC_{pc} may constitute a new tracer for the long-term geochemical impact of DWH in the GOM basin, and perhaps in the North Atlantic.

3.4. DOC Cycling in the Gulf of Mexico Basin

Our results represent the first water column total DOC $\Delta^{14}C$ measurements in the GOM basin. By comparing our Loop Current profiles (LC and LCE) to a Caribbean profile (A20, Station 27; 13°N, 52°W, Figure 2), we discuss a few implications for DOC cycling in the deep GOM basin. LC (P4) surface DOC $\Delta^{14}C$ and $\delta^{13}C$ values and Keeling regression intercepts (Figure S8 and Table S2) suggest marine primary production as the primary source of DOC in the GOM and Caribbean. The nearshore mesoscale surface LCE (P5) profile has generally similar DOC concentrations and isotopic signatures, with surface LCE having only slightly higher DOC and $\Delta^{14}C$ values than the LC—suggesting some possible modern marine DOC production as the LCE moved onshore (Figures 2a–2f and Table S1). At intermediate LC profile depths (350–1000 m), DOC $\Delta^{14}C$ values are higher than A20 values ($\Delta\Delta^{14}C$ = +44‰; Figure 2e and Table S3) suggesting a modern DOC contribution. These higher DOC $\Delta^{14}C$ values may suggest a modern DOC similar to previous work observing higher DIC $\Delta^{14}C$ values in the GOM relative to Atlantic waters attributed to biogenic particle dissolution [*Mathews et al.*, 1973; *Morrison et al.*, 1983]. However, in the LC profile intermediate depths, DOC concentrations are nearly identical to A20 (Figure 2d), suggesting that any additional modern DOC source must in turn be balanced by a removal of aged DOC as this water is transported from the Caribbean to the GOM via the Yucatán Channel.

Finally, deep LC profile DOC concentrations and $\Delta^{14}C$ values were slightly lower than those of A20 by ΔDOC = 1.6 ± 1.0 μM and $\Delta\Delta^{14}C$ = 11 ± 15‰, respectively (Figures 2d and 2e and Table S3). While the errors are high, given deep GOM waters originate in the Caribbean, entering via the Yucatán Channel (sill depth ~ 2040 m), there are three possible reasons for this small negative DOC and $\Delta^{14}C$ offset in the deep LC profile: (1) deep GOM DOC has a long residence time, (2) prevalent natural hydrocarbon seeps contribute some ^{14}C-depleted DOC to the deep GOM, (3) there is removal of young, semilabile DOC with deep water as it advects from the Caribbean to the GOM basin via the Yucatán Channel, or (4) natural variability in deep GOM DOC and $\Delta^{14}C$.

First, aging of DOC could explain the deep P4 offset. A deep DOC $\Delta^{14}C$ offset of ~10‰ suggests an apparent DOC ventilation time of ~150 ^{14}C years. This is ~100 ^{14}C years less than physical advection estimates of GOM basin ventilation of ~250 years [*Rivas et al.*, 2005]. This age offset could indicate a modern DOC source to the deep GOM basin, such as POC solubilization [*Druffel et al.*, 2016; *Follett et al.*, 2014; *Smith et al.*, 1992; *Walker et al.*, 2016b]. This would again be consistent with the above mentioned higher deep GOM DIC $\Delta^{14}C$ values versus the Caribbean Sea. However, we note the variability (± standard error) in deep A20 DOC ^{14}C ages is ±103 years (n = 6). Given the ventilation time of the GOM, variability in these ^{14}C ages likely precludes a DOC residence time estimate. It is also difficult to resolve this offset using DIC $\Delta^{14}C$ since some bomb ^{14}C and tritium is present in the deep Caribbean (Figure S9). Second, while natural oil seeps in the GOM emit up to 140,000 t of hydrocarbon per year [*Kvenvolden and Cooper*, 2003; *Macdonald et al.*, 1993; *Pohlman et al.*, 2011], our DOC concentrations, $\Delta^{14}C$ and $\delta^{13}C$ values, and Keeling regressions (Figure S8) do not indicate a third deep GOM DOC end-member, nor a negative second end-member consistent with hydrocarbon seeps. Although DOC contributions in the immediate vicinity of seeps are possible [*Pohlman et al.*, 2011], our results do not suggest a widespread seep contribution to deep GOM DOC $\Delta^{14}C$ values (see supporting information and Figures S1–S4 and S6). Third, it is possible that DOC is being remineralized during deep water transport

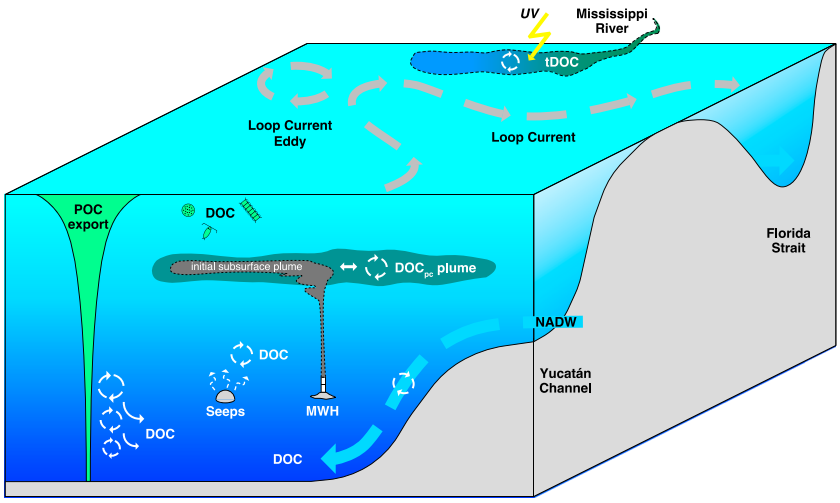

Figure 3. Cartoon depicting the DOC cycle within the Gulf of Mexico (GOM). The Mississippi River discharges terrestrial DOC (tDOC) which is rapidly cycled at the marine interface via photo-oxidation (UV), primary production, and microbial remineralization. Offshore the DOC cycle is dominated by primary production in the surface, slow deep water recharge of North Atlantic Deep Water (NADW), and modern deep DOC (and DIC) contributions from sinking particles. DOC from natural seeps in the deep GOM are not prevalent in DOC isotopic profiles. Thus, seep DOC is most likely labile and quickly remineralized at depth. The isotopic presence of a persistent DOC petrocarbon (DOC_{pc}) plume is observed ~4 years after the Deepwater Horizon spill event at the Macondo wellhead (MWH) site.

between the Caribbean (40.5 ± 0.6 μM; $n = 8$) and GOM basin (38.9 ± 0.8 μM; $n = 4$). An isotopic mass balance of our observed DOC concentration offset of 1.6 ± 1.0 μM suggests a removal of DOC with $\Delta^{14}C = -215 \pm 195‰$. While the uncertainty is high, this mass balance, together with a higher AOU in the deep GOM ($\Delta AOU = 40.1$ μMol L^{-1}; data not shown), suggests a removal of semilabile DOC during transport to the GOM is possible. However, we cannot rule out natural variability in DOC $\Delta^{14}C$, or deep POC solubilization as equally plausible explanations of the deep DOC $\Delta^{14}C$ data.

4. Summary and Implications

These data represent the first total DOC, $\Delta^{14}C$ and $\delta^{13}C$ water column profiles from the GOM and highlight dynamic cycling of DOC within several diverse northern GOM and deep GOM basin environments (Figure 3). A summary of our mass balance and mixing calculation results for each GOM environment are also provided in Table S3. Our results indicate significant export of high $\Delta^{14}C$ tDOC from the Mississippi River. Preliminary $\Delta^{14}C$ evidence of DOC in the deep Mississippi River may indicate a benthic biogenic methane source of exported DOC. A growing body of work suggests photo-oxidation and microbial respiration remove significant tDOC across the Louisiana shelf [*Bianchi et al.*, 2004; *Fichot and Benner*, 2014; *Fichot et al.*, 2014]. Our DOC $\Delta^{14}C$ and $\delta^{13}C$ results also suggest that some marine DOC accumulation occurs at the oceanographic front of the aging Mississippi River plume—consistent with previous work showing phytoplankton bloom and microbially mediated accumulation of semilabile DOC on the LA shelf. Offshore, GOM DOC cycling is dominated by primary production of modern DOC in the surface ocean. Near the Macondo wellhead site, we observe a large mesopelagic anomaly of high DOC with low $\Delta^{14}C$ and $\delta^{13}C$ values. The isotopic presence of a persistent DOC_{pc} plume was observed ~4 years after the Deepwater Horizon spill event. We hypothesize this "preaged," newly added DOC results from the microbial transformation of mesopelagic DWH oil and methane into a natural population of recalcitrant DOC molecules. In the deep GOM basin, DOC $\Delta^{14}C$ values have slightly higher $\Delta^{14}C$ values than deep water recharge sources (i.e., Caribbean and NADW), suggesting some modern deep DOC contributions from sinking particles. Very low DOC $\Delta^{14}C$ values are not observed in the abyssal GOM, suggesting that deep hydrocarbon seep DOC is labile and does not accumulate in the deep GOM basin [*Bianchi et al.*, 2014; *Bracco et al.*, 2016; *Lehr et al.*, 2015, last accessed February; *Mason et al.*, 2016; *McNichol et al.*, 1994; *Strickland*, 1972; *Zhou et al.*, 2013; *Ziervogel et al.*, 2012].

Acknowledgments
We gratefully acknowledge the staff of the Louisiana Universities Marine Consortium (LUMCON) and the crew of the R/V *Pelican* for providing facilities for sampling the Gulf region and seawater DOC collection. We thank Frank Muller-Karger, Daniel Otis, and members of the Institute of Marine Remote Sensing (University of South Florida) for aid in determining the MRP location in near-real time. We also acknowledge Sheila Griffin, Jennifer Walker, Christopher Glynn, and Dachun Zhang (University of California Irvine) for their help with $\Delta^{14}C$ and $\delta^{13}C$ isotopic sample analysis. Matthew Rich (LUMCON) collected and analyzed oxygen and nutrient samples. We thank two anonymous reviewers for their insightful and constructive comments which greatly improved this paper. This work was funded by grants from BP/The Gulf of Mexico Research Initiative (GOMRI) to the Consortium for the Advanced Research of Transport of Hydrocarbon in the Environment (CARTHE; B.E.R.), the Coastal Waters Consortium (CWC; B.J.R.), an American Chemical Society (ACS) Petroleum Research Fund (PRF) New Directions (ND) Grant (E.R.M.D and B.D.W) and a UCI Keck Carbon Cycle AMS Laboratory Postdoctoral Scholarship (B.D.W.). The authors declare no financial conflicts or conflicts of interest. The authors declare that (the/all other) data supporting the findings of this study are available within the article and its supporting information files. Data are also publicly available through the Gulf of Mexico Research Initiative Information and Data Cooperative (GRIIDC) at https://data.gulfresearchinitiative.org (DOI: 10.7266/N7BZ63Z7) and through contacting B.D.W. The funders had no role in the design, execution, or analyses of this project.

References

Beaupre, S. R. (2015), The carbon isotopic composition of marine DOC, in *Biogeochemistry of Dissolved Organic Matter*, edited by D. A. Hansell and C. A. Carlson, pp. 335–368, Elsevier, San Diego, Calif.

Beaupre, S. R., E. R. M. Druffel, and S. Griffin (2007), A low-blank photochemical extraction system for concentration and isotopic analyses of marine dissolved organic carbon, *Limnol. Oceanogr. Methods*, *5*, 174–184.

Bianchi, T. S., T. Filley, K. Dria, and P. G. Hatcher (2004), Temporal variability in sources of dissolved organic carbon in the lower Mississippi River, *Geochim. Cosmochim. Acta*, *68*(5), 959–967.

Bianchi, T. S., C. Osburn, M. R. Shields, S. Yvon-Lewis, J. Young, L. Guo, and Z. Zhou (2014), Deepwater Horizon oil in Gulf of Mexico waters after 2 years: Transformation into the dissolved organic matter pool, *Environ. Sci. Technol.*, *48*(16), 9288–9297.

Bracco, A., J. Choi, K. Joshi, H. Luo, and J. C. McWilliams (2016), Submesoscale currents in the Northern Gulf of Mexico: Deep phenomena and dispersion over the continental slope, *Ocean Modell.*, *101*, 43–58.

Camilli, R., C. M. Reddy, D. R. Yoerger, B. A. S. Van Mooy, M. V. Jakuba, J. C. Kinsey, C. P. McIntyre, S. P. Sylva, and J. V. Maloney (2010), Tracking hydrocarbon plume transport and biodegradation at Deepwater Horizon, *Science*, *330*(6001), 201–204.

Canuel, E. A., and A. K. Hardison (2016), Sources, ages, and alteration of organic matter in estuaries, in *Annual Review of Marine Science*, vol. 8, edited by C. A. Carlson and S. J. Giovannoni, pp. 409–434.

Canuel, E. A., and A. K. Hardison (2016), Sources, ages, and alteration of organic matter in estuaries, *Ann Rev Mar Sci.*, *8*(1), 409–434.

Chanton, J., T. Zhao, B. E. Rosenheim, S. Joye, S. Bosman, C. Brunner, K. M. Yeager, A. R. Diercks, and D. Hollander (2015), Using natural abundance radiocarbon to trace the flux of petrocarbon to the seafloor following the Deepwater Horizon oil spill, *Environ. Sci. Technol.*, *49*(2), 847–854.

Cherrier, J., J. Sarkodee-Adoo, T. P. Guilderson, and J. P. Chanton (2014), Fossil carbon in particulate organic matter in the Gulf of Mexico following the Deepwater Horizon event, *Environ. Sci. Technol. Lett.*, *1*(1), 108–112.

Crespo-Medina, M., M. Crespo-Medina, C. D. Meile, R. M. W. Amon, A. Bracco, J. P. Montoya, T. A. Villareal, and A. M. Wood (2014), The rise and fall of methanotrophy following a deepwater oil-well blowout, *Nat. Geosci.*, *7*(6), 423–427.

D'Souza, N. A., A. Subramaniam, A. R. Juhl, M. Hafez, A. Chekalyuk, S. Phan, B. Yan, I. R. MacDonald, S. C. Weber, and J. P. Montoya (2016), Elevated surface chlorophyll associated with natural oil seeps in the Gulf of Mexico, *Nat. Geosci.*, *9*(3), 215–218.

Druffel, E. R. M., S. Griffin, A. I. Coppola, and B. D. Walker (2016), Radiocarbon in dissolved organic carbon of the Atlantic Ocean, *Geophys. Res. Lett.*, *43*, 5279–5286, doi:10.1002/2016GL068746.

Druffel, E. R. M., S. Griffin, B. D. Walker, A. I. Coppola, and D. S. Glynn (2013), Total uncertainty of radiocarbon measurements of marine dissolved organic carbon and methodological recommendations, *Radiocarbon*, *55*(2–3), 1135–1141.

Duan, S. W., T. S. Bianchi, and T. P. Sampere (2007), Temporal variability in the composition and abundance of terrestrially-derived dissolved organic matter in the lower Mississippi and Pearl Rivers, *Mar. Chem.*, *103*(1–2), 172–184.

Dunn, D. D. (1996), Trends in nutrient inflows to the Gulf of Mexico from streams draining the conterminous United States 1972–1993, Rep. 96–4113, prepared in cooperation with the U.S. Austin, Texas: Environmental Protection Agency, Gulf of Mexico Program, Nutrient Enrichment Issue Committee, U.S. Geological Survey.

Fichot, C. G., and R. Benner (2014), The fate of terrigenous dissolved organic carbon in a river-influenced ocean margin, *Global Biogeochem. Cycles*, *28*, 300–318, doi:10.1002/2013GB004670.

Fichot, C. G., S. E. Lohrenz, and R. Benner (2014), Pulsed, cross-shelf export of terrigenous dissolved organic carbon to the Gulf of Mexico, *J. Geophys. Res. Oceans*, *119*, 1176–1194, doi:10.1002/2013JC009424.

Follett, C. L., D. J. Repeta, D. H. Rothman, L. Xu, and C. Santinelli (2014), Hidden cycle of dissolved organic carbon in the deep ocean, *Proc. Natl. Acad. Sci. U.S.A.*, *111*(47), 16,706–16,711.

Gardner, W. S., R. Benner, R. M. W. Amon, J. B. Cotner, J. F. Cavaletto, and J. R. Johnson (1996), Effects of high-molecular-weight dissolved organic matter on nitrogen dynamics in the Mississippi River plume, *Mar. Ecol. Prog. Ser.*, *133*(1–3), 287–297.

Graham, W. M., R. H. Condon, R. H. Carmichael, I. D'Ambra, H. K. Patterson, L. J. Linn, and F. J. Hernandez Jr. (2010), Oil carbon entered the coastal planktonic food web during the Deepwater Horizon oil spill, *Environ. Res. Lett.*, *5*(4).

Griffin, S., S. R. Beaupre, and E. R. M. Druffel (2010), An alternate method of diluting dissolved organic carbon seawater samples for ^{14}C analysis, *Radiocarbon*, *52*(2–3), 1224–1229.

Guo, L., D. M. White, C. Xu, and P. H. Santschi (2009), Chemical and isotopic composition of high-molecular-weight dissolved organic matter from the Mississippi River plume, *Mar. Chem.*, *114*(3–4), 63–71.

Hansell, D. A., C. A. Carlson, D. J. Repeta, and R. Schlitzer (2009), Dissolved organic matter in the ocean—A controversy stimulates new insights, *Oceanography*, *22*(4), 202–211.

Joye, S. B., A. P. Teske, and J. E. Kostka (2014), Microbial dynamics following the Macondo oil well blowout across Gulf of Mexico environments, *Bioscience*, *64*(9), 766–777.

Joye, S. B., I. R. MacDonald, I. Leifer, and V. Asper (2011a), Magnitude and oxidation potential of hydrocarbon gases released from the BP oil well blowout, *Nat. Geosci.*, *4*(3), 160–164.

Joye, S. B., et al. (2011b), Comment on "A persistent oxygen anomaly reveals the fate of spilled methane in the deep Gulf of Mexico", *Science*, *332*(6033).

Kessler, J. D., et al. (2011), A persistent oxygen anomaly reveals the fate of spilled methane in the deep Gulf of Mexico, *Science*, *331*(6015), 312–315.

Kleindienst, S., S. Grim, M. Sogin, A. Bracco, M. Crespo-Medina, and S. B. Joye (2016), Diverse, rare microbial taxa responded to the Deepwater Horizon deep-sea hydrocarbon plume, *ISME J.*, *10*(2), 400–415.

Kvenvolden, K. A., and C. K. Cooper (2003), Natural seepage of crude oil into the marine environment, *Geo-Mar. Lett.*, *23*(3–4), 140–146.

Lehr, W., S. Bristol, and A. Possolo (2015), Federal Interagency Solutions Group, Oil budget calculator science and engineering team, Oil Budget Calculator.

Macdonald, I. R., N. L. Guinasso, S. G. Ackleson, J. F. Amos, R. Duckworth, R. Sassen, and J. M. Brooks (1993), Natural oil slicks in the Gulf of Mexico visible from space, *J. Geophys. Res.*, *98*(C9), 16,351–16,364, doi:10.1029/93JC01289.

MacDonald, I. R., et al. (2015), Natural and unnatural oil slicks in the Gulf of Mexico, *J. Geophysical Res. Oceans*, *120*, 8364–8380, doi:10.1002/2015JC011062.

Mason, O. U., E. J. Canter, L. E. Gillies, T. K. Paisie, and B. J. Roberts (2016), Mississippi River plume enriches microbial diversity in the northern Gulf of Mexico, *Front. Microbiol.*, *7*.

Mathews, T. D., A. D. Fredericks, and W. M. Sachett (1973), The geochemistry of radiocarbon in the Gulf of Mexico, Rep. 725–734 pp, International Atomic Energy Agency (IAEA): IAEA., Vienna.

McNichol, A. P., and L. I. Aluwihare (2007), The power of radiocarbon in biogeochemical studies of the marine carbon cycle: Insights from studies of dissolved and particulate organic carbon (DOC and POC), *Chem. Rev.*, *107*(2), 443–466.
McNichol, A. P., G. A. Jones, D. L. Hutton, A. R. Gagnon, and R. M. Key (1994), The rapid preparation of seawater ΣCO_2 for radiocarbon analysis at the National Ocean Sciences AMS Facility, *Radiocarbon*, *36*(2), 237–246.
Morrison, J. M., W. J. Merrell, R. M. Key, and T. C. Key (1983), Property distributions and deep chemical measurements within the Western Gulf of Mexico, *J. Geophys. Res.*, *88*(NC4), 2601–2608, doi:10.1029/JC088iC04p02601.
Paris, C. B., M. L. Hénaff, Z. M. Aman, A. Subramaniam, J. Helgers, D.-P. Wang, V. H. Kourafalou, and A. Srinivasan (2012), Evolution of the Macondo well blowout: Simulating the effects of the circulation and synthetic dispersants on the subsea oil transport, *Environ. Sci. Technol.*, *46*(24), 13,293–13,302.
Pohlman, J., J. Bauer, W. Waite, C. Osburn, and N. Chapman (2011), Methane hydrate-bearing seeps as a source of aged dissolved organic carbon to the oceans, *Nat. Geosci.*, *4*(1), 37–41.
Pohlman, J. W., J. E. Bauer, E. A. Canuel, K. S. Grabowski, D. L. Knies, C. S. Mitchell, M. J. Whiticar, and R. B. Coffin (2009), Methane sources in gas hydrate-bearing cold seeps: Evidence from radiocarbon and stable isotopes, *Mar. Chem.*, *115*(1–2), 102–109.
Reddy, C. M., et al. (2012), Composition and fate of gas and oil released to the water column during the Deepwater Horizon oil spill, *Proc. Natl. Acad. Sci. U.S.A.*, *109*(50), 20229–20234.
Rivas, D., A. Badan, and J. Ochoa (2005), The ventilation of the deep Gulf of Mexico, *J. Phys. Oceanogr.*, *35*(10), 1763–1781.
Rousset, C., and L. M. Beal (2010), Observations of the Florida and Yucatan currents from a Caribbean cruise ship, *J. Phys. Oceanogr.*, *40*(7), 1575–1581.
Rousset, C., and L. M. Beal (2014), Closing the transport budget of the Florida Straits, *Geophys. Res. Lett.*, *41*, 2460–2466, doi:10.1002/2014GL059498.
Santschi, P. H., L. D. Guo, M. Baskaran, S. Trumbore, J. Southon, T. S. Bianchi, B. Honeyman, and L. Cifuentes (1995), Isotopic evidence for the contemporary origin of high-molecular-weight organic-matter in oceanic environments, *Geochim. Cosmochim. Acta*, *59*(3), 625–631.
Shen, Y., C. Fichot, and R. Benner (2012), Floodplain influence on dissolved organic matter composition and export from the Mississippi-Atchafalaya River system to the Gulf of Mexico, *Limnol. Oceanogr.*, *57*(4), 1149–1160.
Shen, Y., C. Fichot, S. Liang, and R. Benner (2016), Biological hot spots and the accumulation of marine dissolved organic matter in a highly productive ocean margin, *Limnol. Oceanogr.*, *61*(4), 1287–1300.
Smith, D. C., M. Simon, A. L. Alldredge, and F. Azam (1992), Intense hydrolytic enzyme activity on marine aggregates and implications for rapid particle dissolution, *Nature*, *359*(6391), 139–142.
Southon, J., G. Santos, K. Druffel-Rodriguez, E. Druffel, S. Trumbore, X. M. Xu, S. Griffin, S. Ali, and M. Mazon (2004), The Keck Carbon Cycle AMS laboratory, University of California, Irvine: Initial operation and a background surprise, *Radiocarbon*, *46*(1), 41–49.
Strickland, J. (1972), *A Practical Handbook of Seawater Analysis*, *Fisheries Research Board of Canada*, vol. 167, 2nd ed., p. 310, Minister of Supply and Services Canada, Ottawa, Canada.
Taylor, J. R. (1997), *An Introduction to Error Analysis: The Study of Uncertainties in Physical Measurements*, 2nd ed., Univ. Science Books, Saussalito, Calif.
Valentine, D. L., et al. (2010), Propane respiration jump-starts microbial response to a deep oil spill, *Science*, *330*(6001), 208–211.
Vogel, J. S., J. R. Southon, and D. E. Nelson (1987), Catalyst and binder effects in the use of filamentous graphite for AMS, *Nucl. Instrum. Methods Phys. Res. Sect. B-Beam Inter. Mater. Atoms*, *29*(1–2), 50–56.
Walker, B. D., S. Griffin, and E. R. M. Druffel (2016b), Effect of acidified versus frozen storage on marine dissolved organic carbon concentration and isotopic composition, *Radiocarbon*, 1–15.
Walker, B. D., S. R. Beaupre, T. Guilderson, M. McCarthy, and E. R. M. Druffel (2016a), Pacific carbon cycling constrained by organic matter size, age, and composition relationships, *Nat. Geosci.*, *9*, 888–891.
Xu, X. M., S. E. Trumbore, S. H. Zheng, J. R. Southon, K. E. McDuffee, M. Luttgen, and J. C. Liu (2007), Modifying a sealed tube zinc reduction method for preparation of AMS graphite targets: Reducing background and attaining high precision, *Nucl. Instrum. Methods Phys. Res. Sect. B-Beam Inter. Mater. Atoms*, *259*(1), 320–329.
Zhou, Z., L. Guo, A. M. Shiller, S. E. Lohrenz, V. L. Asper, and C. L. Osburn (2013), Characterization of oil components from the Deepwater Horizon oil spill in the Gulf of Mexico using fluorescence EEM and PARAFAC techniques, *Mar. Chem.*, *148*, 10–21.
Ziervogel, K., L. McKay, B. Rhodes, C. L. Osburn, J. Dickson-Brown, C. Arnosti, and A. Teske (2012), Microbial activities and dissolved organic matter dynamics in oil-contaminated surface seawater from the Deepwater Horizon oil spill site, *PLoS One*, *7*(4).